

Near-threshold η production in pp collisions

Qi-Fang Lü and De-Min Li*

Department of Physics, Zhengzhou University, Zhengzhou, Henan 450001, China

We study near-threshold η meson production in pp collisions within an effective Lagrangian approach combined with the isobar model, by allowing for the various intermediate nucleon resonances due to the π , η , and ρ -meson exchanges. It is shown that the ρ -meson exchange is the dominant excitation mechanism for these resonances, and the contribution from the $N^*(1720)$ is dominant. The total cross section data can be reasonably reproduced, and the anisotropic angular distributions of the emitted η meson are consistent with experimental measurements. Besides, the invariant mass spectra of pp and $p\eta$ explain the data well at excess energy of 15 MeV, and are basically consistent with the data at excess energy of 40 MeV. However, our model calculations cannot reasonably account for the two-peak structure in the $p\eta$ distribution at excess energies of 57 and 72 MeV, which suggests that a more complicated mechanism is needed at higher energy region.

PACS numbers: 13.75.Cs; 14.20.Gk; 13.30.Eg

I. INTRODUCTION

The properties of hadrons are subject to the behavior of quantum chromodynamics (QCD) in the non-perturbative region, so the study of hadrons is important to deepen the understanding of the non-perturbative properties of QCD. Meson production reactions in nucleon-nucleon collisions near threshold are a good platform to obtain new information on the hadrons and therefore have received a lot of attentions both experimentally and theoretically in recent years [1]. A large set of experimental data on η meson production in the $pp \rightarrow pp\eta$ [2–10], $pn \rightarrow d\eta$, and $pn \rightarrow pn\eta$ reactions [11–14] has been accumulated, which has stimulated many theoretical investigations on η meson production [15–34].

η meson production in NN collisions is generally assumed to occur predominantly through

*Electronic address: lidm@zzu.edu.cn

re-scattering of the intermediate nucleon resonances caused by the meson exchanges. For this basic mechanism, it is not yet clear which of the possible nucleon resonances plays the dominant role. For example, in Refs. [15–19, 22–28] it is suggested that the $N^*(1535)$ is dominant, while in Ref. [33] it is found that the $N^*(1520)$ is dominant and the $N^*(1535)$ contribution is small due to the strong destructive interference among the exchanged mesons. Also, it is not yet clear which of the possible meson exchanges plays the most important role. For example, in Refs. [15, 22, 32] it is claimed that the pseudoscalar mesons π and η exchanges are dominant, whereas in Refs. [16, 19, 24, 25] it is suggested that vector meson ρ exchange is dominant. In Ref. [27] it is found that both the π exchange and the ρ exchange can describe the cross sections well. The study on the $N^*(1535)N\rho$ coupling in the framework of an effective Lagrangian approach manifests that the value of $g_{N^*(1535)N\rho}$ is strong [35], which favors the importance of the ρ meson exchange in NN collisions.

In Ref. [34], the final state interaction (FSI) enhancement factor is considered and it is found that the measured pp and ηp effective mass spectra can be well reproduced by allowing for a linear energy dependence in the leading ${}^3P_0 \rightarrow {}^1S_0, s$ partial wave amplitude.

In Ref. [8] it is suggested that the higher partial waves may be important even at 15.5 MeV. Besides the $N^*(1535)$, the ρ meson may also couple strongly to other higher resonances. The large branching ratio and the small phase space for the $N^*(1720) \rightarrow N\rho$ also suggest that the $N^*(1720)N\rho$ coupling is strong.

With the inspiration of the factors mentioned above, we shall restudy the $pp \rightarrow pp\eta$ reaction in an effective Lagrangian approach combined with the isobar model. The combination of the effective Lagrangian approach and the isobar model turns out to be a good method to study hadron resonance production in the πN , NN , and $\bar{K}N$ scattering [22, 32, 33, 35–40]. In the present work, we assume that the near threshold η meson production in proton-proton collisions is through the intermediate $N^*(1535)$, $N^*(1650)$, $N^*(1710)$, $N^*(1720)$, and the nucleon pole caused by the π , η , and ρ mesons exchanges. The proton-proton FSI and proton- η FSI are also considered.

This work is organized as follows. The basic formalism and ingredients used in our model are given in Section II. The numerical results and discussions are given in Section III. A summary is given in Section IV.

II. FORMALISM AND INGREDIENTS

The basic tree level Feynman diagrams for the $pp \rightarrow pp\eta$ reaction are shown in Fig. 1.

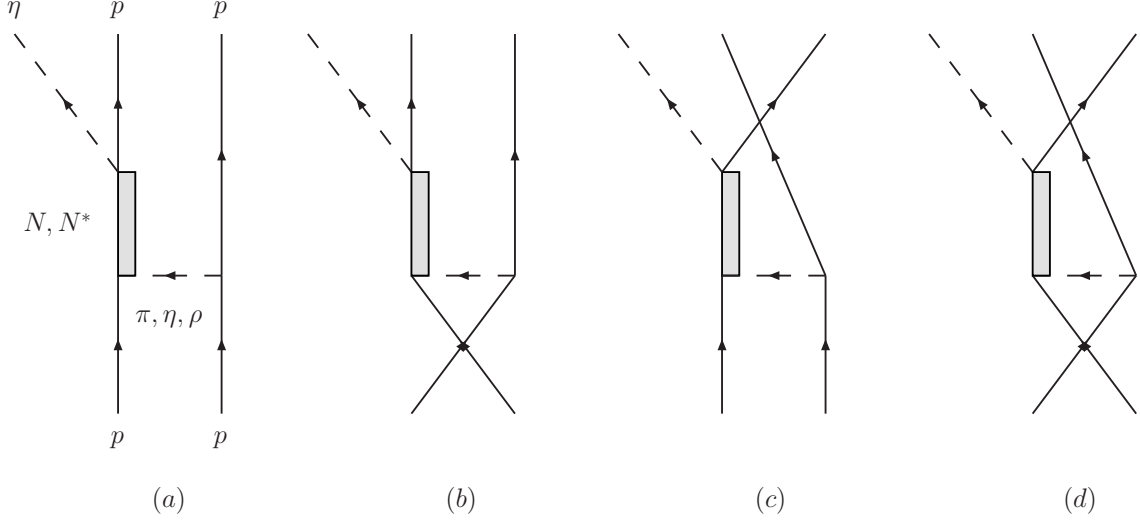


FIG. 1: Feynman diagrams for the $pp \rightarrow pp\eta$ reaction.

The interaction Lagrangians for the πNN , ηNN and ρNN couplings can be written as [36, 37]:

$$\mathcal{L}_{\pi NN} = -ig_{\pi NN}\bar{\psi}_N\gamma_5\vec{\tau} \cdot \vec{\pi}\psi_N, \quad (1)$$

$$\mathcal{L}_{\eta NN} = -ig_{\eta NN}\bar{\psi}_N\gamma_5\eta\psi_N, \quad (2)$$

$$\mathcal{L}_{\rho NN} = -g_{\rho NN}\bar{\psi}_N \left(\gamma_\mu + \frac{\kappa}{2m_N}\sigma_{\mu\nu}\partial^\nu \right) \vec{\tau} \cdot \vec{\rho}^a\psi_N. \quad (3)$$

The effects of the non-point-like structures of exchanged mesons are taken into account by introducing the following off-shell form factors in the MNN vertexes[41–43]

$$F_M^{NN}(k_M^2) = \left(\frac{\Lambda_M^2 - m_M^2}{\Lambda_M^2 - k_M^2} \right)^n, \quad (4)$$

where M denotes the exchanged meson; $n = 1$ for $\pi^0 NN$ and ηNN vertexes, $n = 2$ for the $\rho^0 NN$ vertex; k_M , m_M , and Λ_M are the 4-momentum, mass, and cut-off parameter, respectively, for the exchanged-meson M . The relevant parameters used in our calculations are: $g_{\pi NN}^2/4\pi = 14.4$, $g_{\eta NN}^2/4\pi = 0.4$, $g_{\rho NN}^2/4\pi = 0.9$, $\kappa = 6.1$ [36, 37, 41–48], $\Lambda_\rho = 1.85$ GeV [36, 37], and $\Lambda_\pi = \Lambda_\eta = 0.8$ GeV.

The following interaction Lagrangians involving the nucleon resonances N^* can be obtained within a Lorentz covariant orbital-spin (L-S) scheme for the N^*NM couplings [49]:

$$\mathcal{L}_{\pi NN^*(1535)} = ig_{\pi NN^*(1535)}\bar{\psi}_N\vec{\tau} \cdot \vec{\pi}\psi_{N^*(1535)} + h.c., \quad (5)$$

$$\mathcal{L}_{\eta NN^*(1535)} = ig_{\eta NN^*(1535)} \bar{\psi}_N \eta \psi_{N^*(1535)} + h.c., \quad (6)$$

$$\mathcal{L}_{\rho NN^*(1535)} = ig_{\rho NN^*(1535)} \bar{\psi}_N \gamma_5 \left(\gamma_\mu - \frac{q_\mu \not{q}}{q^2} \right) \vec{\tau} \cdot \vec{\rho}^\mu(p_\rho) \psi_{N^*(1535)} + h.c., \quad (7)$$

$$\mathcal{L}_{\pi NN^*(1650)} = ig_{\pi NN^*(1650)} \bar{\psi}_N \vec{\tau} \cdot \vec{\pi} \psi_{N^*(1650)} + h.c., \quad (8)$$

$$\mathcal{L}_{\eta NN^*(1650)} = ig_{\eta NN^*(1650)} \bar{\psi}_N \eta \psi_{N^*(1650)} + h.c., \quad (9)$$

$$\mathcal{L}_{\rho NN^*(1650)} = ig_{\rho NN^*(1650)} \bar{\psi}_N \gamma_5 \left(\gamma_\mu - \frac{q_\mu \not{q}}{q^2} \right) \vec{\tau} \cdot \vec{\rho}^\mu(p_\rho) \psi_{N^*(1650)} + h.c., \quad (10)$$

$$\mathcal{L}_{\pi NN^*(1710)} = -ig_{\pi NN^*(1710)} \bar{\psi}_N \gamma_5 \vec{\tau} \cdot \vec{\pi} \psi_{N^*(1710)} + h.c., \quad (11)$$

$$\mathcal{L}_{\eta NN^*(1710)} = -ig_{\eta NN^*(1710)} \bar{\psi}_N \gamma_5 \eta \psi_{N^*(1710)} + h.c., \quad (12)$$

$$\mathcal{L}_{\rho NN^*(1710)} = -g_{\rho NN^*(1710)} \bar{\psi}_N \left(\gamma_\mu + \frac{\kappa}{2m_N} \sigma_{\mu\nu} \partial^\nu \right) \vec{\tau} \cdot \vec{\rho}^\mu \psi_{N^*(1710)} + h.c., \quad (13)$$

$$\mathcal{L}_{\pi NN^*(1720)} = g_{\pi NN^*(1720)} \bar{\psi}_N \vec{\tau} \cdot \partial^\mu \vec{\pi} \psi_{N^*(1720)\mu} + h.c., \quad (14)$$

$$\mathcal{L}_{\eta NN^*(1720)} = g_{\eta NN^*(1720)} \bar{\psi}_N \partial^\mu \eta \psi_{N^*(1720)\mu} + h.c., \quad (15)$$

$$\mathcal{L}_{\rho NN^*(1720)} = g_{\rho NN^*(1720)} \bar{\psi}_N \gamma_5 \vec{\tau} \cdot \vec{\rho}^\mu \psi_{N^*(1720)\mu} + h.c.. \quad (16)$$

At the N^*NM vertexes, the monopole form factors are employed:

$$F_M^{N^*N}(k_M^2) = \frac{\Lambda_M^{*2} - m_M^2}{\Lambda_M^{*2} - k_M^2}. \quad (17)$$

With the effective Lagrangians listed above, the partial width of the nucleon resonance N^* can be derived. From the experimental data on the partial width of the corresponding nucleon resonance, the N^*NM coupling constants can be obtained. For the N^* resonance below the $N\rho$ threshold, the partial decay width $\Gamma_{N^* \rightarrow N\rho \rightarrow N\pi\pi}$ is employed to determine the $N^*N\rho$ coupling constant [36, 37]. The relevant coupling constants and cut-off parameters are listed in Table I.

For the nucleon pole N and nucleon resonances N^* , the following form factors are used [37, 51–53]:

$$F_N(q^2) = \frac{\Lambda_N^4}{\Lambda_N^4 + (q^2 - m_N^2)^2}, \quad (18)$$

$$F_{N^*}(q^2) = \frac{\Lambda_{N^*}^4}{\Lambda_{N^*}^4 + (q^2 - M_{N^*}^2)^2}, \quad (19)$$

with $\Lambda_N = 1.0$ GeV and $\Lambda_{N^*} = 2.0$ GeV.

The meson propagators used in our calculation are:

$$G_{\pi/\eta}(k_{\pi/\eta}) = \frac{i}{k_{\pi/\eta}^2 - m_{\pi/\eta}^2}, \quad (20)$$

TABLE I: Relevant parameters of the nucleon resonances used in our calculation. The widths and branching ratios are taken from the PDG [50].

Resonance	Width(GeV)	Decay channel	Branching ratios	$g^2/4\pi$	Cut-off(GeV)
$N^*(1535)$	0.15	$N\pi$	0.45	0.037	0.8
		$N\eta$	0.42	0.28	0.8
		$N\rho$	0.02	5.55	0.8
$N^*(1650)$	0.15	$N\pi$	0.70	0.052	1.5
		$N\eta$	0.10	0.036	1.5
		$N\rho$	0.01	0.0064	1.5
$N^*(1710)$	0.1	$N\pi$	0.125	0.072	1.5
		$N\eta$	0.20	0.97	1.5
		$N\rho$	0.15	0.019	1.5
$N^*(1720)$	0.25	$N\pi$	0.11	0.11	1.5
		$N\eta$	0.04	0.35	1.5
		$N\rho$	0.775	635.11	1.5

$$G_{\rho}^{\mu\nu}(k_{\rho}) = -i \left(\frac{g^{\mu\nu} - k_{\rho}^{\mu}k_{\rho}^{\nu}/k_{\rho}^2}{k_{\rho}^2 - m_{\rho}^2} \right). \quad (21)$$

The propagators of the N^* resonances can be written as

$$G_{N^*}(q) = \frac{\not{q} + M_{N^*}}{q^2 - M_{N^*}^2 + iM_{N^*}\Gamma_{N^*}}, \quad (22)$$

for spin- $\frac{1}{2}$ resonances, and

$$G_{N^*}^{\mu\nu}(q) = \frac{-P_{\mu\nu}(q)}{q^2 - M_{N^*}^2 + iM_{N^*}\Gamma_{N^*}}, \quad (23)$$

with

$$P_{\mu\nu}(q) = -(\not{q} + M_{N^*}) \left[g_{\mu\nu} - \frac{1}{3}\gamma_{\mu}\gamma_{\nu} - \frac{1}{3M_{N^*}}(\gamma_{\mu}q_{\nu} - \gamma_{\nu}q_{\mu}) - \frac{2}{3M_{N^*}^2}q_{\mu}q_{\nu} \right], \quad (24)$$

for spin- $\frac{3}{2}$ resonances.

As usual, in Eq. (22) the following energy-dependent total width of the $N^*(1535)$ resonance, $\Gamma_{N^*(1535)}(s)$, is employed [54],

$$\Gamma_{N^*(1535)}(s) = \Gamma_{N^*(1535) \rightarrow N\pi} \frac{\rho_{\pi N}(s)}{\rho_{\pi N}(M_{N^*(1535)}^2)} + \Gamma_{N^*(1535) \rightarrow N\eta} \frac{\rho_{\eta N}(s)}{\rho_{\eta N}(M_{N^*(1535)}^2)}, \quad (25)$$

where the two-body phase space factor $\rho_{\pi(\eta)N}(s)$ is

$$\rho_{\pi(\eta)N}(s) = \frac{2p_{\pi(\eta)N}^{cm}(s)}{\sqrt{s}} = \frac{\sqrt{[s - (m_N + m_{\pi(\eta)})^2][s - (m_N - m_{\pi(\eta)})^2]}}{s}. \quad (26)$$

The invariant amplitude for the nucleon pole N or nucleon resonances N^* can be expressed as

$$\mathcal{M}^{N/N^*} = \sum_{i=\pi, \eta, \rho} \mathcal{M}_i^{N/N^*}, \quad (27)$$

$$\mathcal{M}_i^{N/N^*} = \sum_{j=a, b, c, d} \eta_j \mathcal{M}_{i,j}^{N/N^*}, \quad (28)$$

where $\eta_a = \eta_d = 1$ and $\eta_b = \eta_c = -1$. The explicit expressions of $\mathcal{M}_{i,j}^{N/N^*}$ can be derived straightforwardly according to the Feynman rules. For example, $\mathcal{M}_{\pi,a}^{N^*(1535)}$ can be written as

$$\begin{aligned} \mathcal{M}_{\pi,a}^{N^*(1535)} &= g_{\pi NN} g_{\pi NN^*(1535)} g_{\eta NN^*(1535)} F_{\pi}^{NN}(k_{\pi}^2) F_{\pi}^{N^*(1535)N}(k_{\pi}^2) F_{N^*(1535)}(q^2) \\ &\quad \times G_{\pi}(k_{\pi}) \bar{u}(p_3, s_3) \gamma_5 u(p_2, s_2) \bar{u}(p_4, s_4) G_{N^*(1535)}(q) u(p_1, s_1), \end{aligned} \quad (29)$$

where s_i ($i = 1, 2, 3, 4$) and p_i ($i = 1, 2, 3, 4$) represent the spin projection and 4-momentum of the two initial and two final protons, respectively.

The pp FSI and $p\eta$ FSI are taken into account by introducing the following enhancement factors

$$F_{pp}(k_{pp}) = \frac{k_{pp} + i\beta}{k_{pp} - i\alpha}, \quad (30)$$

$$F_{p\eta}(k_{p\eta}) = \frac{1}{1 - ik_{p\eta}a}, \quad (31)$$

where k_{pp} and $k_{p\eta}$ are the internal momenta of the pp and $p\eta$ subsystems, respectively. The relevant parameters are: $\alpha = 0.1 \text{ fm}^{-1}$, $\beta = 0.5 \text{ fm}^{-1}$ [55], and $a = (0.487 + i0.171) \text{ fm}$ [52, 53]. The overall final state interaction is the product of these enhancements [29, 55]:

$$F_{FSI} = F_{pp}(k_{pp}) F_{\eta p}(k_{\eta p_3}) F_{\eta p}(k_{\eta p_4}), \quad (32)$$

where p_3 and p_4 denote the two final protons.

With the modular square of the full invariant amplitude $|\mathcal{M}|^2 = \sum_{N, N^*} |\mathcal{M}^{N/N^*} F_{FSI}|^2$, the differential cross section for the $pp \rightarrow pp\eta$ reaction can be written as

$$d\sigma(pp \rightarrow pp\eta) = \frac{1}{4} \frac{m_p^2}{F} \sum_{s_i} \sum_{s_f} |\mathcal{M}|^2 \frac{m_p d^3 p_3}{E_3} \frac{m_p d^3 p_4}{E_4} \frac{d^3 p_5}{2E_5} \frac{1}{2} \delta^4(p_1 + p_2 - p_3 - p_4 - p_5), \quad (33)$$

where F is the flux factor

$$F = (2\pi)^5 \sqrt{(p_1 \cdot p_2)^2 - m_p^4}. \quad (34)$$

The factor $\frac{1}{2}$ before the δ function in Eq. (33) comes from the two identical protons in the final states. The interference terms between different resonances are ignored.

III. NUMERICAL RESULTS AND DISCUSSIONS

With a Monte Carlo multi-particle phase space integration program, the total cross section versus excess energy ε up to 80 MeV, the invariant mass spectra, angular distributions, and Dalitz plots at excess energies $\varepsilon = 15, 40, 57,$ and 72 MeV for the $pp \rightarrow pp\eta$ reaction are calculated.

The total cross section is shown in Fig. 2 together with the experimental data. Our results agree fairly well with the experimental data. From Fig. 2, one can see that the contributions from the t-channel ρ and π -meson exchanges are important and the ρ exchange plays the dominant role, but the contribution from the η -meson exchange is negligible. Fig. 2 also shows that the contributions from the $N^*(1720)$ and $N^*(1535)$ are important and the $N^*(1720)$ plays the dominant role. The contribution of the $N^*(1535)$ is smaller than that of the $N^*(1720)$ due to the strong destructive interference among the exchange mesons, which is similar to the result of Ref. [33]. The contributions from the $N^*(1650)$ and $N^*(1710)$ are negligible.

The invariant mass spectra, angular distribution, and Dalitz plot at excess energy $\varepsilon = 15$ MeV are shown in Fig. 3 together with experimental data. The measured pp and $p\eta$ invariant mass spectra and the angular distribution of η are reproduced well. From Fig. 3 (a) and (d), one can see that the pp FSI plays an important role.

The invariant mass spectra, angular distribution, and Dalitz plot at excess energy $\varepsilon = 40$ MeV as well as the experimental data are shown in Fig. 4. For the invariant mass spectra of proton-proton and proton- η , the theoretical results are in agreement with the experimental data except for those near the proton-proton (proton- η) threshold. This small discrepancy indicates the pp FSI used in our calculation may be somewhat strong in this region.

For the angular distribution of the emitted η meson in the overall c.m. frame, there are two groups of data which do not agree with each other [8, 57]. One is isotropic [57], while the other is anisotropic [8], as shown in Fig. 4 (c). Our result indicates that the angular distribution

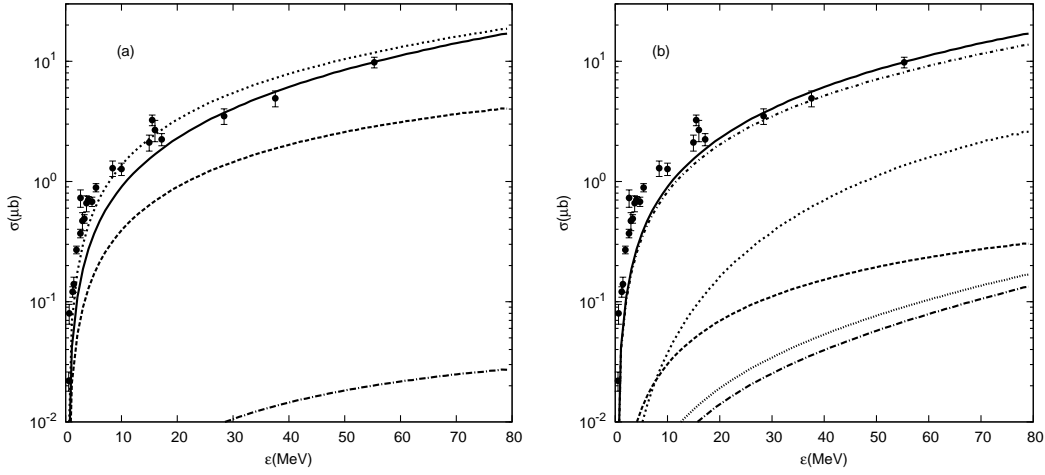


FIG. 2: Total cross section vs excess energy ε for the $pp \rightarrow pp\eta$ reaction from the present calculation (solid curves) are compared with experimental data [2–7, 56–59]. (a): The dashed, dotted, and dashed-dotted lines stand for contributions from the π , ρ , and η -meson exchanges, respectively. (b): The dashed, dotted, short-dotted, dashed-dotted, and dot-short-dashed lines stand for contributions from the N , $N^*(1535)$, $N^*(1650)$, $N^*(1710)$, and $N^*(1720)$, respectively.

of the η meson is anisotropic, consistent with the data from Ref. [8]. As pointed out by Ref. [8, 17, 58], the anisotropy is probably due to a mainly destructive interference between the dominant ρ exchange and π exchange. It is interesting to point out that the $N^*(1535)$ dominant interpretations [22, 28, 60] give almost isotropic angular distribution of the η at this region except that Ref. [27] gives the anisotropic angular distribution of the η by allowing for contributions from baryonic and mesonic currents.

The invariant mass spectra, angular distribution, and Dalitz plot at excess energy $\varepsilon = 72$ MeV as well as the experimental data are shown in Fig. 5. The experimental data shown in Fig. 5 (a) indicate the pp FSI should be rather weak, so the pp FSI is ignored in this energy region. This rough procedure has been used in double-pion production in nucleon-nucleon collisions and the results turn out to be considerably improved [61]. Our pp invariant mass spectrum can reasonably account for the data.

The two-peak structure in the proton- η distribution cannot be reproduced in our calculation, which is similar to the result from Ref. [33]. This suggests that the structure in the $p\eta$ distribution cannot be simply interpreted by the $N^*(1535)$, $N^*(1650)$, $N^*(1710)$, and $N^*(1720)$ resonances, and a more complicated mechanism is strongly called for.

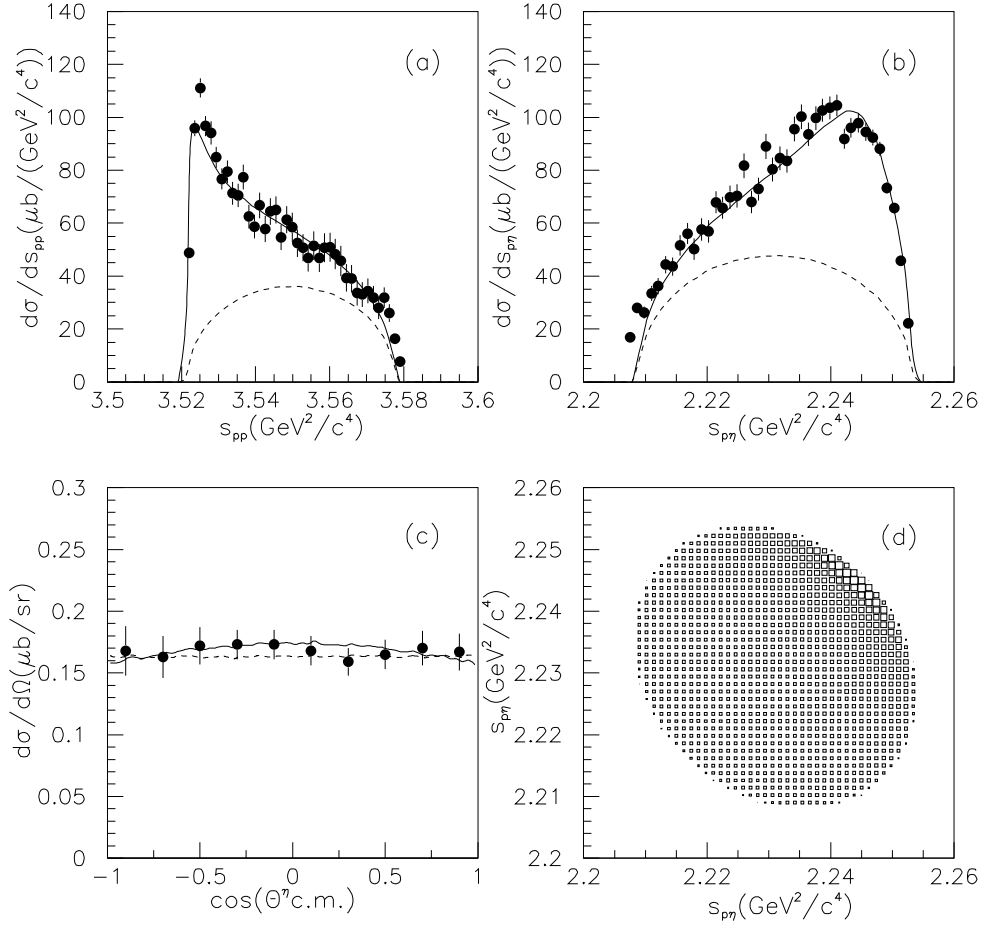


FIG. 3: Differential cross sections (solid lines) and Dalitz plot for the $pp \rightarrow pp\eta$ reaction at the excess energy of $\varepsilon = 15$ MeV compared with the experimental data [56, 57] and phase space distribution (dashed lines). (a) Distribution of the square of proton-proton invariant mass; (b) Distribution of the square of proton- η invariant mass; (c) Angular distribution of the emitted η meson in the c.m. frame of the total system; (d) Dalitz plot.

Our angular distribution of the η at $\varepsilon = 72$ MeV again indicates that the η distribution is anisotropic, consistent with the data from Ref. [8]. To our knowledge, there is as yet no theoretical paper for addressing the angular distribution of the η at this region.

The invariant mass spectra, angular distribution, and Dalitz plot at excess energy $\varepsilon = 57$ MeV as well as preliminary experimental data are shown in Fig. 6. Similar to the case at excess energy $\varepsilon = 72$ MeV, the preliminary data of Ref. [62] show that the two-peak structure appears in the proton- η distribution and the angular distribution of the η is anisotropic. Our predicted

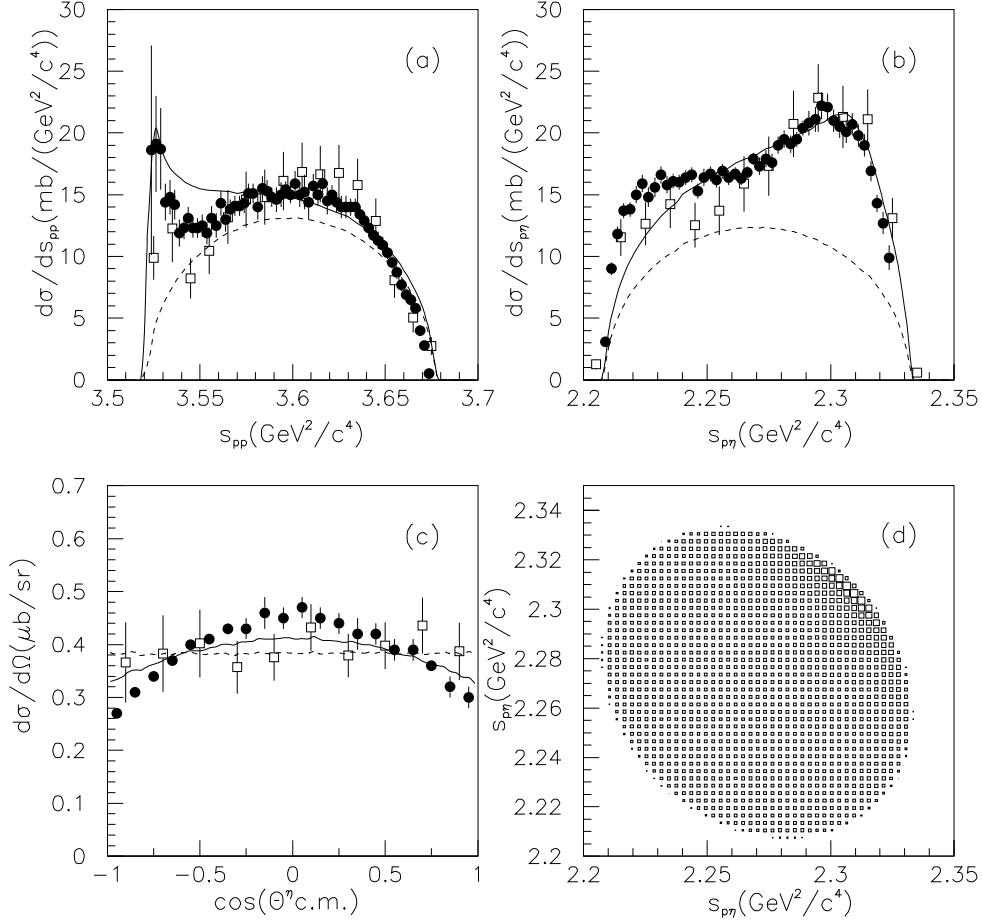


FIG. 4: Same as Fig. 3 but at excess energy of $\varepsilon = 40$ MeV. Experimental data are taken from Ref. [57] (squares) and Ref. [8] (dots).

angular distribution for the η at $\varepsilon = 57$ MeV is anisotropic, consistent with the data. However, the $p\eta$ invariant mass distribution shows large differences between the present model and the experimental data.

It is noted that our present model does not include the higher partial waves for the $p\eta$ FSI. As pointed out by Refs. [8, 63], the experimental data indicate the higher partial waves at higher reaction energies could be important. The contributions of the higher partial waves being neglected in the current model calculations may cause the discrepancy between the experimental data and our model of the proton- η distribution at excess energies $\varepsilon = 57$ and 72 MeV.

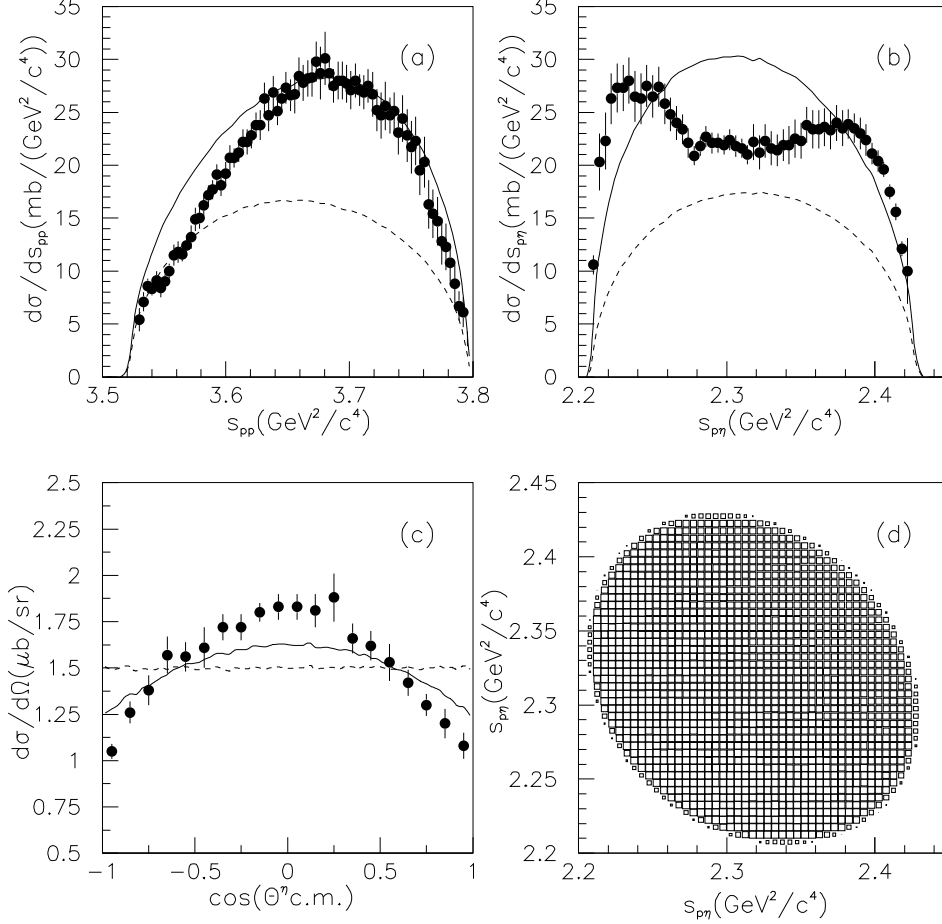


FIG. 5: Same as Fig. 3 but at excess energy of $\varepsilon = 72$ MeV, and with pp FSI ignored. Experimental data are taken from Ref. [8].

IV. SUMMARY AND CONCLUSIONS

In this paper we have calculated the $pp \rightarrow pp\eta$ reaction within an effective Lagrangian approach combined with the isobar model. Our model calculations can reasonably reproduce the total cross sections up to excess energy of 80 MeV.

It is shown that for the $pp \rightarrow pp\eta$ reaction, the contribution of the ρ -meson exchange is larger than that of the π -meson exchange, and the contribution of the $N^*(1720)$ is larger than that of the $N^*(1535)$.

Also, the same cut-off parameters for the $N^*(1650)$, $N^*(1710)$, and $N^*(1720)$ resonances are used, which makes it suitable to investigate the relative contributions of the $N^*(1650)$,

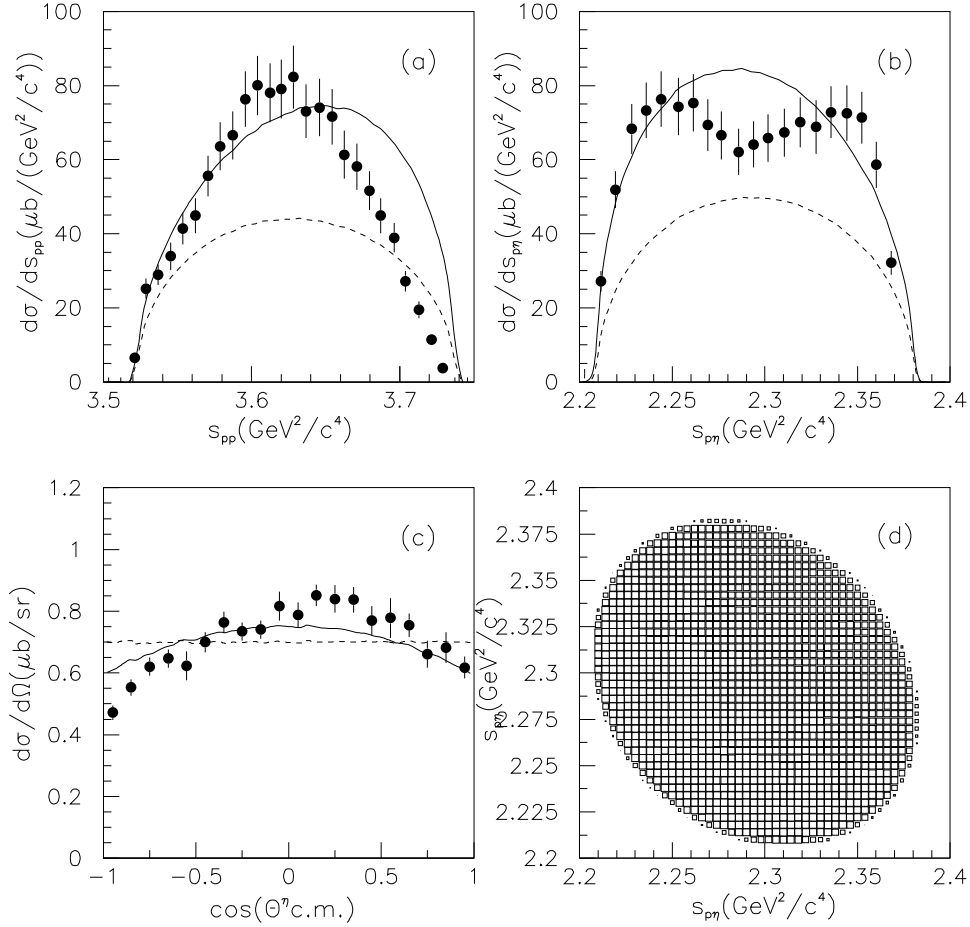


FIG. 6: Same as Fig. 3 but at excess energy of $\varepsilon = 57$ MeV, and with pp FSI ignored. Experimental data are taken from Ref. [62].

$N^*(1710)$, and $N^*(1720)$ resonances. Our results show that the contributions from the $N^*(1650)$ and $N^*(1710)$ are negligible.

Our calculations can reasonably explain the measured pp and $p\eta$ invariant mass spectra at excess energies $\varepsilon = 15$ and 40 MeV, but fail to explain the two-peak structure in the proton- η distribution at excess energies $\varepsilon = 57$ and 72 MeV, which suggests that in the higher energy region, a more complicated mechanism is needed.

We give the anisotropic angular distribution of the η at $\varepsilon = 40$, 57 and 72 MeV, consistent with the data from Refs. [8, 62]. This favors the interpretation that the interference between the ρ exchange and π exchange is mainly destructive.

Acknowledgement

We thank Dr. Ju-Jun Xie for helpful discussions and valuable suggestions. This work is partly supported by the National Natural Science Foundation of China under grant 11105126.

-
- [1] C. Hanhart, Phys. Rept. **397**, 155 (2004).
 - [2] A. M. Bergdolt *et al.*, Phys. Rev. D **48**, R2969 (1993).
 - [3] E. Chiavassa *et al.*, Phys. Lett. B **322**, 270 (1994).
 - [4] H. Calén *et al.*, Phys. Lett. B **366**, 39 (1996).
 - [5] F. Hibou *et al.*, Phys. Lett. B **438**, 41 (1998).
 - [6] J. Smyrski *et al.*, Phys. Lett. B **474**, 182 (2000).
 - [7] G. Agakishiev *et al.*, Eur. Phys. J. A **48**, 74 (2012).
 - [8] H. Petrén *et al.*, Phys. Rev. C **82**,055206 (2010).
 - [9] R. Czyżykiewicz *et al.*, Phys. Rev. Lett. **98**, 122003 (2007)
 - [10] C. Pauly, Ph. D. thesis, University of Hamburg (2006).
 - [11] H. Calén *et al.*, Phys. Rev. Lett. **79**, 2642 (1997).
 - [12] H. Calén *et al.*, Phys. Rev. C **58**, 2667 (1998).
 - [13] H. Calén *et al.*, Phys. Rev. Lett. **80**, 2069 (1998);
 - [14] P. Moskal *et al.*, Phys. Rev. C **79**, 015208 (2009).
 - [15] M. Batinić, A. Svarc, and T.-S. H. Lee, Physica Scripta, **56**, 321 (1997).
 - [16] A. Moalem, E. Gedalin, L. Razdolskaya, and Z. Shorer, Nucl. Phys. A **600**, 445 (1996).
 - [17] J. F. Germond and C. Wilkin, Nucl. Phys. A **518**, 308 (1990).
 - [18] J. M. Laget, F. Wellers, and J. F. Lecomte, Phys. Lett. B **257**, 254 (1991).
 - [19] T. Vetter, A. Engel, T. Biró, and U. Mosel, Phys. Lett. B **263**, 153 (1991).
 - [20] B. L. Alvaredo and E. Oset, Phys. Lett. B **324**, 125 (1994).
 - [21] M. T. Pena, H. Garcilazo, and D.O. Riska, Nucl. Phys. A **683** 322 (2001).
 - [22] R. Shyam, Phys. Rev. C **75**, 055201 (2007).
 - [23] E. Gedalin, A. Moalem, and L. Razdolskaya, Nucl. Phys. A **634**, 368 (1998).
 - [24] A. B. Santra and B. K. Jain, Nucl. Phys. A **634**, 309 (1998).
 - [25] G. Fäldt and C. Wilkin, Physica Scripta, **64**, 427 (2001).
 - [26] V. Baru *et al.*, Phys. Rev. C **67**, 024002 (2003).

- [27] K. Nakayama, J. Speth, and T.-S. H. Lee, Phys. Rev. C **65**, 045210 (2002).
- [28] K. Nakayama, J. Haidenbauer, C. Hanhart, and J. Speth, Phys. Rev. C **68**, 045201 (2003).
- [29] V. Bernard, N. Kaiser, and Ulf-G. Meissner, Eur. Phys. J. A **4**, 259 (1999).
- [30] P. Moskal, M. Wolke, A. Khokkaz, and W. Oelert, Prog. Part. Nucl. Phys. **49**, 1 (2002).
- [31] D. O. Riska and G. Brown, Nucl. Phys. A **679**, 577 (2001).
- [32] X. Cao and X. G. Lee, Phys. Rev. C **78**, 035207 (2008).
- [33] K. Nakayama, Y. Oh, and H. Haberzettl, J. Korean Phys. Soc. **59**, 224 (2011).
- [34] A. Deloff, Phys. Rev. C **69**, 035206 (2004).
- [35] J. J. Xie, C. Wilkin, and B. S. Zou, Phys. Rev. C **77**, 058202 (2008).
- [36] J. J. Xie and B.S. Zou, Phys. Lett. B **649**, 405 (2007).
- [37] J. J. Xie, B. S. Zou, and H. Q. Chaing, Phys. Rev. C **77**, 015206 (2008).
- [38] Q. F. Lü, X. H. Liu, J. J. Xie, and D. M. Li, Mod. Phys. Lett. A **29**,1450012 (2014).
- [39] Q. F. Lü, J. J. Xie, and D. M. Li, Phys. Rev. C **90**,034002 (2014).
- [40] Q. F. Lü, R. Wang, J. J. Xie, X. R. Chen, and D. M. Li, arXiv:1412.6272.
- [41] R. Machleidt, K. Holinde, and C. Elster, Phys. Rep. **149**, 1 (1987).
- [42] R. Machleidt, Adv. Nucl. Phys. **19**, 189 (1989).
- [43] R. Brockmann and R. Machleidt, Phys. Rev. C **42**, 1965 (1990).
- [44] K. Tsushima, S. W. Huang, and A. Faessler, Phys. Lett. B **337**, 245 (1994)
- [45] K. Tsushima, A. Sibirtsev, and A. W. Thomas, Phys. Lett. B **390**, 29 (1997).
- [46] K. Tsushima, A. Sibirtsev, A. W. Thomas, and G. Q. Li, Phys. Rev. C **59**, 369 (1999), Erratum-
ibid. C **61**, 029903 (2000).
- [47] A. Sibirtsev and W. Cassing, nucl-th/9802019.
- [48] A. Sibirtsev, K. Tsushima, W. Cassing, and A. W. Thomas, Nucl. Phys. A **646**, 427 (1999).
- [49] B. S. Zou and F. Hussain, Phys. Rev. C **67**, 015204 (2003).
- [50] K. A. Olive *et al.* (Particle Data Group), Chin. Phys. C **38**, 090001 (2014).
- [51] G. Penner and U. Mosel, Phys. Rev. C **66**, 055211 (2002); *ibid.* C **66**, 055212 (2002);
V. Shklyar, H. Lenske and U. Mosel, Phys. Rev. C **72**, 015210 (2005).
- [52] T. Feuster and U. Mosel, Phys. Rev. C **58**, 457 (1998).
- [53] T. Feuster and U. Mosel, Phys. Rev. C **59**, 460 (1999).
- [54] W. H. Liang, P. N. Shen, J. X. Wang, and B. S. Zou, J. Phys. G **28**, 333 (2002).
- [55] Y. Maeda *et al.*, Phys. Rev. C **77**, 015204 (2008).

- [56] P. Moskal *et al.*, Phys. Rev. C **69**, 025203 (2004).
- [57] M. Abdel-Bary *et al.*, Eur. Phys. J. A **16**, 127 (2003).
- [58] H. Calen *et al.*, Phys. Lett. B **458**, 190 (1999).
- [59] F. Balestra *et al.*, Phys. Rev. C **69**, 064003 (2004).
- [60] A. Fix and H. Arenhoevel, Phys. Rev. C **69**, 014001 (2004).
- [61] X. Cao, B. S. Zou, and H. S. Xu, Phys. Rev. C **81**, 065201 (2010).
- [62] N. Shah [WASA-at-COSY Collaboration], AIP Conf. Proc. **1374**, 402 (2011).
- [63] B. Krusche and C. Wilkin, Prog. Part. Nucl. Phys. **80**, 43 (2014).